Desalination and Water Treatment
www.deswater.com

doi: 10.5004/dwt.2023.29357

289 (2023) 206–220
March

Simultaneous removal of Methylene Blue and Direct Blue 71 with Pb(II) ions from multi-component systems: application of the multi-component Langmuir model

Görkem Polat[a], Ezgi Türkeş[a], Yeşim Sağ Açıkel[b,*]

[a]*Bioengineering Division, Institute of Science, Hacettepe University, Ankara, Turkey, email: gorkem.polat@hacettepe.edu.tr (G. Polat), ezgi.turkes@hacettepe.edu.tr (E. Türkeş)*
[b]*Chemical Engineering Department and Bioengineering Division, Faculty of Engineering, Hacettepe University, Ankara, Turkey, Tel.: +90 312 297 74 44; email: yesims@hacettepe.edu.tr*

Received 17 September 2022; Accepted 1 February 2023

ABSTRACT

This study aims to investigate the simultaneous removal of Methylene Blue (MB), Direct Blue 71 (DB71), and Pb(II) ions, which are frequently found together at high concentrations in different industrial wastewaters, such as textile, paper, leather, paint, and plastic manufacturing wastewaters. The simultaneous removal of Pb(II) ions with MB and DB71 from binary mixtures was investigated by the adsorption method. Magnetic halloysite nanotubes-alginate (MHNTs-ALG) hybrid beads were used to remove these components from the binary adsorption media. For this purpose, a magnetic property was gained to halloysite nanotubes using the "co-precipitation method". Magnetic halloysite nanotubes (MHNTs) were composited with alginate (ALG) biopolymers through the "extrusion dripping method". The adsorption capacities and efficiency of these synthesized MHNTs-ALG hybrid beads were investigated according to their anionic and cationic pollutant content in binary mixtures, and the synergistic and antagonistic effects of these components on each other were investigated by comparing them according to single systems. The compatibility with the multi-component Langmuir adsorption model for binary systems was examined using equilibrium adsorption data, and the values of the constants showing the adsorption capacity and affinity were calculated. In binary mixtures of Pb(II)-MB, the maximum amounts of Pb(II) and MB adsorbed per unit adsorbent weight calculated from the multi-component Langmuir model were 248.46 mg/g ($q_{Pb,m}$) and 946.92 mg/g ($q_{MB,m}$), respectively. The maximum adsorption capacities of Pb(II) and Direct Blue 71 from binary systems were determined as 203.14 mg/g ($q_{Pb,m}$) and 118.96 mg/g ($q_{DB71,m}$), respectively. The co-presence of Pb(II) and MB was concluded to create a synergistic effect compared to the adsorption of Pb(II) ions alone and an antagonistic effect compared to the adsorption of MB alone. The co-presence of Pb(II) and DB71 was observed to form a synergistic effect compared to the individual presence of Pb(II) ions and an antagonistic-synergistic mixed effect compared to the individual presence of DB71.

Keywords: Multi-component adsorption; Magnetic halloysite nanotubes-alginate hybrid beads; Pb(II); Methylene Blue; Direct Blue 71; Multi-component Langmuir model

1. Introduction

Synthetic dyes are commonly used in the leather, paper, and textile industries. Toxicity and carcinogenic effects on aquatic life are observed due to releasing these dyes into water without treatment, which leads to significant environmental problems [1]. Due to their complex chemical structure, these dyes are resistant to degradation by chemical,

* Corresponding author.

physical, and biological processes [2]. Various methods, such as flocculation, precipitation, membrane filtration, and electrochemical techniques, have been developed to remove these pollutants from dye-containing media. Among these methods, the adsorption process is highly preferred because of its simplicity and low energy consumption [3–5].

Various adsorbents (agricultural wastes, clay, fly ash, perlite, activated carbon, etc.) are used to remove dyes from wastewater by adsorption. The adsorbents selected for the adsorption process are expected to be cost-effective and biodegradable [6]. Biopolymers come into prominence in the adsorption method due to their biodegradability, environmental compatibility, and low costs. Biopolymeric alginate (ALG) is a material composed of many hydroxyl and carboxyl groups, is biodegradable, and contains α-L-guluronic acid and β-D-mannuronic acid groups. Due to these anionic groups in its structure, it is a highly effective material in removing cationic pollutants [7]. ALG, a water-soluble natural alginic acid salt, is a linear polysaccharide extracted from brown algae. There are studies in the literature on creating composite forms with natural materials, which would increase strength due to the low mechanical strength of ALG [8–11]. Halloysite nanotubes (HNTs) used to prepare composite beads are aluminosilicate clays with a hollow nanotubular structure. HNTs ($Al_2Si_2O_5(OH)_4 \cdot nH_2O$) have excellent properties due to their wide surface areas, pore volumes, and hydroxyl groups in their structure [12–15]. When HNTs are added to the structure of ALG beads, they enhance this structure's thermal, chemical, mechanical strength, and adsorption capacity and increase its affinity to cationic-anionic compounds [16,17]. A magnetic property was also gained to HNTs using the "co-precipitation method" [18,19]. Magnetic halloysite nanotubes (MHNTs) were composited with alginate (ALG) biopolymers through the "extrusion dripping method". The easy removal of Magnetic halloysite nanotubes-alginate (MHNTs-ALG) hybrid beads prepared this way from aqueous media was ensured without precipitation and centrifugation, and the particles' mechanical and thermal strength was further improved. Thus, the restriction on the individual use of ALG beads in packed column-type reactors due to the weakness of their mechanical properties and their swelling at low pH and on the individual use of HNTs in the same reactors due to their nano-dimensions was eliminated.

Dyes and heavy metals are usually present together in wastewater. It is extremely important for these materials, which will be used in treatment, to have an affinity for both cationic and anionic pollutants and be able to ensure simultaneous adsorption from media containing multiple pollutants [20]. Methylene Blue (MB), commonly known as Basic Blue 9, is a cationic soluble dye that decomposes as chloride ions and cations in aqueous solutions and turns into green/blue powder or crystal solid [21,22]. Although MB is frequently used in medicine, biology, and chemistry, it is known to have harmful effects on humans and the environment because of its solubility in water. Azo dyes compose a key group of synthetic dyes widely used in textile industries, with about a 50% share of total dyes used worldwide. MB is an azo dye with a heterocyclic aromatic cation structure used in the printing and dyeing process. An average dye concentration has been reported to be up to 300 mg/L in the effluent generated from the textile industry. A 10–250 mg/L dye concentration has also been reported, but it is less frequently encountered. Studies in the literature have also reported dye concentrations as high as 1,500 mg/L in some textile effluents. These textile effluents also contain a range of metal ions, such as lead, chromium, cobalt, copper, iron, manganese, and nickel [23]. Heavy metals arise from pretreatment, dyeing, printing, and finishing steps due to the use of metal-containing chemicals, catalysts, oxidizing agents, fixing agents, cross-linking agents, etc. Heavy metals have a high density exceeding 5 mg/cm^3. Lead (Pb) is one of the heavy metal ions often found in textile effluents due to its use in producing pigments for textile dyeing. Pb(II) is one of the three most toxic metals. MB and Pb(II) ions are present together, particularly in the wastewater of paint and plastic manufacturing, the textile dyeing industry, and mining and lead battery companies. Direct Blue 71 (DB71), another dye, is a bluish-gray powder classified as a dye with anionic properties when dissolved in water [24]. DB71 is an azo dye group with three azo bonds. Direct dyes constitute about 17% of all dyes used for dyeing textiles and about 30% of dyes used for dyeing cellulose fiber [25]. It is often preferred in the textile, paper, leather, and nylon industries. It yields good results, especially in dyeing textile products with high fibrous cellulose content [25]. It is carcinogenic due to the azo groups in its structure [26,27]. Lead and lead acetate are used in fiber production as a dyeing auxiliary/mordant in textile processing. Lead acetate is used in coloring, dyeing, and printing as an oxidizing/reducing agent [28]. Binary mixtures of Pb(II) ions and dye pollutants are formed as a result of careless wastewater disposal procedures. Therefore, it is important to obtain an effective adsorbent that can remove Pb(II) ions and anionic and cationic dyes together.

Some studies emphasize that Pb(II) and MB pollutions exist together but use sea plants such as *Posidonia oceanica* [29] and adsorbents such as magnetic carbonate hydroxyapatite/graphene oxide [30] and mesoporous coral limestones [31] to remove these pollutants from single-component systems. Studies on DB71 pollution alone are quite rare, and the removal of DB71 alone from aqueous media has been achieved with organic compost (food waste compost) [32], wheat husk [3], and pistachio hull wastes [26]. The aforementioned studies investigated the fit of the removal of Pb(II) and dyes from aqueous media to single-component adsorption equilibrium and kinetic models. The presence of the other component in the medium in binary mixtures creates synergistic and antagonistic effects on the adsorption capacity of the sorbent and changes the values of adsorption equilibrium constants. The presence of the other component may create an antagonistic effect on the adsorption capacity of a certain component and reduce it compared to a single-component system. However, the total adsorption capacity of the sorbent may increase according to the condition of each component alone; in this case, the total effect is synergistic. In the literature, very few studies have been published on the fit of binary heavy metal ion-dye adsorption equilibrium to multi-component adsorption models. Some studies have investigated the competitive adsorption of the Pb(II)-MB binary system to various adsorbents [33–35]. In these studies, the maximum adsorption capacities obtained for Pb(II) and MB have been compared with the Pb(II) and

MB competitive adsorption capacities of MHNTs-ALG hybrid beads. To the best of our knowledge, the simultaneous adsorption of the Pb(II)-DB71 binary system has not been studied in the literature to date. In this study, adsorption from binary mixtures containing Pb(II)-MB and Pb(II)-DB71 through MHNTs-ALG hybrid beads was carried out. The fit of the adsorption equilibrium from the binary mixtures of Pb(II) ions and dyes to the multi-component Langmuir model was examined, and the values of the competitive and/or partially competitive adsorption constants were calculated.

2. Adsorption isotherm models

Adsorption isotherm models provide important information about physicochemical parameters, adsorption mechanism, surface properties, and the degree of affinity of adsorbents with thermodynamic assumptions [36]. Different versions of these equilibrium isotherm models exist for single and multiple-system adsorption [37].

The multi-component Langmuir adsorption model used in this study includes the same assumptions as the single-component Langmuir model. The Langmuir model, developed for competitive adsorption, assumes that there is a homogeneous surface relative to adsorption energy, there is no interaction between the adsorbed types, and all adsorption sites are equally present for all adsorbed types. The N-component Langmuir model can be defined as follows [38]:

$$q_{i,\mathrm{eq}} = \frac{q_{i,m} \times K_{i,L} \times C_{i,\mathrm{eq}}}{1 + \sum_{j=1}^{N} K_{j,L} \times C_{j,\mathrm{eq}}} \tag{1}$$

According to this model, $q_{i,m}$: adsorption capacity (mg/g) when the adsorbent surface is coated with a single layer of component i; $K_{i,L}$; $K_{j,L}$: Langmuir constant (L/mg), which is related to adsorption energy and shows the affinity of the adsorbent for components i and j; $K_i = K_{0i\exp}(Q/RT)$; $C_{i,\mathrm{eq}}$ $C_{j,\mathrm{eq}}$: concentration remaining at equilibrium without being adsorbed for components i and j (mg/L); $q_{i,\mathrm{eq}}$; $q_{i,\mathrm{eq}}$: amount adsorbed per unit adsorbent weight at equilibrium for components i and j (mg/g).

To reliably evaluate the validity of isotherm model forms (i.e., the goodness of fit between $q_{\mathrm{eq,meas.}}$ and $q_{\mathrm{eq,pred.}}$), three error functions [average relative error (ARE), average absolute error (EABS), and average relative standard error (ARSE)] were employed.

2.1. Average relative error

The ARE model, which shows a tendency to underestimate or overestimate the experimental data, tries to minimize fractional error distribution within the entire concentration range examined [36,37].

$$\mathrm{ARE} = \frac{100}{n} \sum_{i=1}^{n} \left| \frac{q_{\mathrm{eq,meas.}} - q_{\mathrm{eq,pred.}}}{q_{\mathrm{eq,meas.}}} \right|_i \tag{2}$$

where $q_{\mathrm{eq,meas.}}$: amount of Pb(II)/dye adsorbed per unit adsorbent weight at equilibrium (mg/g); $q_{\mathrm{eq,pred.}}$: amount of Pb(II)/dye adsorbed per unit adsorbent weight calculated from adsorption isotherm models (mg/g).

2.2. Average absolute error

According to the EABS, an increase in errors causes a tendency toward high-concentration data and ensures a better fit [36,37].

$$\mathrm{EABS} = \frac{1}{n} \sum_{i=1}^{n} \left| q_{\mathrm{eq,meas.}} - q_{\mathrm{eq,pred.}} \right|_i \tag{3}$$

2.3. Average relative standard error

The ARSE was calculated using the equation [39].

$$\mathrm{ARSE} = \sqrt{\frac{1}{n-1} \sum_{i=1}^{n} \left(\frac{q_{\mathrm{eq,meas.}} - q_{\mathrm{eq,pred.}}}{q_{\mathrm{eq,meas.}}} \right)_i^2} \tag{4}$$

2.4. Sum of squared errors

Adsorption isotherm parameter estimates were calculated by non-linear least-squares regression analysis, minimizing the sum of squared errors (SSE) [37,39]:

$$\mathrm{SSE} = \sum_{i=1}^{n} \left(q_{\mathrm{eq,meas.}} - q_{\mathrm{eq,pred.}} \right)^2 \tag{5}$$

where n is the number of experimental measurements, and $q_{\mathrm{eq,meas.}}$ and $q_{\mathrm{eq,pred.}}$ are the measured and predicted equilibrium adsorption capacities, respectively.

2.5. Total standard deviation

The total standard deviation was calculated using the following equation:

$$\mathrm{Total\ Standard\ Deviation}\left(\mathrm{TSD}\right) = \sum_{i=1}^{n} \left(q_{\mathrm{eq,meas.}i} - \overline{q_{\mathrm{eq}}} \right)^2 \tag{6}$$

where $q_{\mathrm{eq,meas.}}$ and $\overline{q_{\mathrm{eq}}}$ are the measured and average measured equilibrium adsorption capacities, respectively.

3. Materials and methods

3.1. Preparation of MHNTs-ALG

To prepare MHNTs-ALG hybrid beads, a magnetic property was first gained to HNTs using the "co-precipitation method". $FeCl_2{\cdot}4H_2O$ and $FeCl_3{\cdot}6H_2O$ iron salts were added to HNTs, dispersed in distilled water in a five-necked reactor, at a ratio of 1:2 in the nitrogen atmosphere. MHNTs were synthesized by slowly adding NH_4OH to the mixture heated to 80°C. After the prepared MHNTs were dried in a vacuum oven, certain amounts of MHNTs and ALG were mixed in pure water using the "extrusion dripping" technique, and MHNTs-ALG hybrid beads were synthesized by adding the mixture to the $CaCl_2$ solution in a dropwise manner. After washing the beads, they were dried in a freeze-dryer. The preparation and detailed characterization studies of MHNTs and MHNTs-ALG hybrid

beads (dimension analysis with scanning electron microscopy, transmission electron microscopy, Zetasizer, Fourier-transform infrared spectroscopy, thermogravimetric analysis, Brunauer–Emmett–Teller, and vibrating sample magnetometer) have been described elaborately in our previous publication [19].

3.2. Adsorption studies in binary mixtures (containing Pb-MB and Pb-DB71)

The most appropriate conditions for the removal of Pb(II) ions [19] and MB dye [40] from single-component systems with MHNTs-ALG hybrid beads have been determined in our previous studies. Since both components exhibit cationic properties, the most appropriate adsorption conditions are similar. In adsorption studies conducted with binary systems of Pb(II) ions and cationic MB dye, hybrid beads with a 1:2 mass ratio of MHNTs to ALG, where both components were adsorbed the most in single systems, were used. 12.5 mg of hybrid beads were added to 25 mL of adsorption media with an optimum adsorption pH adjusted to 5 for both components. To investigate the fit of the binary adsorption data to the multi-component Langmuir model, the initial concentration of Pb(II) ions was increased in the range of 50–500 mg/L, whereas the concentration of MB dye was kept constant at 50, 150, 250, 400, and 500 mg/L in each adsorption medium.

Since MHNTs-ALG hybrid beads are predominantly a negative matrix, in the medium containing Pb(II), the conditions of the adsorption medium were adjusted to the optimum adsorption conditions obtained previously for the single-component DB71 with the same matrix to achieve partial selectivity for the anionic DB71 dye [41]. In the binary adsorption studies of Pb(II) ions–anionic DB71 dye, hybrid beads (6.25 mg) with a mass ratio of MHNTs to ALG of 3:2 were used, the optimum adsorption pH for DB71 was adjusted to 3.0 in the medium, and the study was carried out in a 25 mL solution medium. To examine the fit of the binary adsorption data to the multi-component Langmuir model, the initial concentration of Pb(II) ions was increased in the range of 50–250 mg/L, whereas the concentration of DB71 dye was kept constant at 50, 100, 150, 200, and 250 mg/L in each adsorption medium.

4. Results and discussion

4.1. Pb(II)-MB and Pb(II)-DB71 binary system adsorption studies in batch stirred reactors

Adsorption studies with binary systems are more complicated due to the competition and surface interactions of the adsorbed components. The properties of binary and single systems differ. The interaction in the active regions of the adsorbent changes with the characteristics of the heavy metal ion and the dye. The surface interaction may differ depending on the adsorption mechanism and whether the reaction is reversible.

4.1.1. Pb(II) ion-MB adsorption studies

In the adsorption studies conducted with the binary systems of Pb(II) ions and cationic MB dye, hybrid beads with a 1:2 mass ratio of MHNTs to ALG, where both components were adsorbed the most in single systems, were used [19,40]. 12.5 mg of hybrid beads were added to 25 mL of the adsorption media, whose pH was set to 5. The media were prepared to contain Pb(II) ions and MB at different concentrations. While the initial concentration of Pb(II) ions was increased in the range of 50–500 mg/L, the concentration of MB dye was kept constant at 0, 50, 150, 250, 400, and 500 mg/L in each adsorption medium. Fig. 1 shows the change in the equilibrium adsorption concentration of Pb(II) ions, $C_{Pb,ads.}$ (mg/g), with initial Pb(II) ion concentration.

As seen in Fig. 1, the concentration of Pb(II) ions adsorbed at equilibrium, $C_{Pb,ads.}$ (mg/L), increased with the increasing initial concentrations of Pb(II) ions. On the other hand, the adsorbed Pb(II) ion concentration decreased compared to the single-component system and with the increase in the MB concentration. This indicates that the active regions of the adsorbent start to close with the increasing MB concentration. The maximum adsorbed Pb(II) ion concentration and adsorption capacity at equilibrium (the amount of adsorbed Pb(II) ions per unit weight of MHNTs-ALG at equilibrium), $q_{Pb,eq.}$ (mg/g), were obtained as 145.87 mg/L and 250.9 mg/g in the medium containing 500 mg/L of Pb(II) and 50 mg/L of MB, respectively. The adsorbed Pb(II) ion concentration and adsorption capacity at the lowest equilibrium were 124.48 mg/L and 214.10 mg/g in the medium containing 500 mg/L of Pb(II) and 500 mg/L of MB, respectively.

Fig. 2 shows the change in the adsorption efficiency of Pb(II) ions, $Y_{Pb,eff.}$ (%), with the increasing initial Pb(II) ion concentration at MB concentrations varying between 0–500 mg/L. It is observed that the adsorption efficiency of Pb(II) ions decreased with both increasing Pb(II) ion concentration and increasing MB concentration. The highest Pb(II) adsorption efficiency was obtained as 88.45% at a 50 mg/L Pb(II) ion concentration in a medium containing 50 mg/L of MB. Pb(II) adsorption efficiency decreased to 24.86% in the medium containing 500 mg/L of Pb(II) and 500 mg/L of MB.

Fig. 3 presents the change in the MB concentration adsorbed at equilibrium, $C_{MB,ads.}$ mg/L, with the initial MB

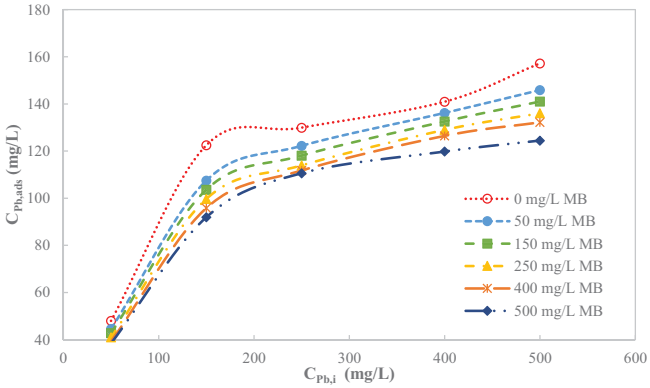

Fig. 1. The change in the Pb(II) ion concentration adsorbed at equilibrium with the increasing initial Pb(II) ion concentration in media containing MB at different concentrations in the Pb(II)-MB binary adsorption system (temperature: 25°C, solution volume: 25 mL, pH: 5.0, adsorbent amount: 12.5 mg, MHNTs-ALG mass ratio: 1:2).

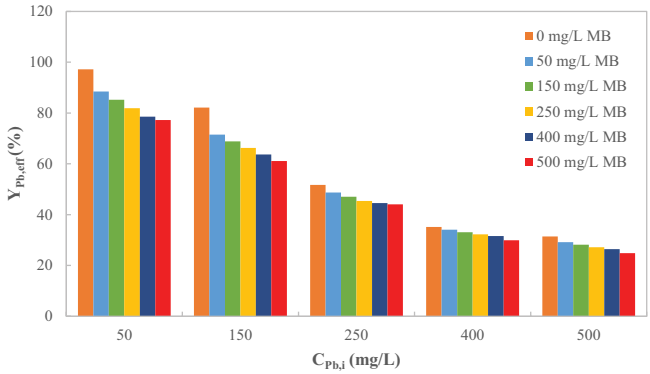

Fig. 2. The change in Pb(II) ion adsorption efficiency with the increasing initial Pb(II) ion concentration in media containing MB at different concentrations in the Pb(II)-MB binary adsorption system (temperature: 25°C, solution volume: 25 mL, pH: 5.0, adsorbent amount: 12.5 mg, MHNTs-ALG mass ratio: 1:2).

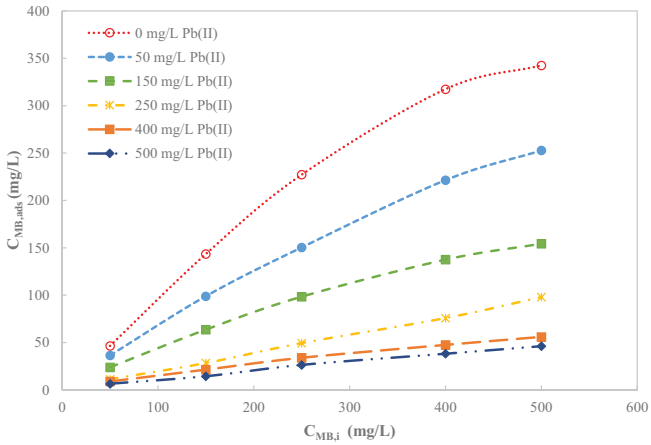

Fig. 3. The change in the MB concentration adsorbed at equilibrium with the increasing initial MB concentration in media containing Pb(II) ions at different concentrations in the Pb(II)-MB binary adsorption system (temperature: 25°C, solution volume: 25 mL, pH: 5.0, adsorbent amount: 12.5 mg, MHNTs-ALG ratio: 1:2).

concentration by increasing the MB concentration in the range of 50–500 mg/L in media containing 0, 50, 150, 250, 400, and 500 mg/L Pb(II) ions. The individual MB adsorption capacity of MHNTs-ALG beads is significantly higher compared to the single-component Pb(II) system. Moreover, the presence of Pb(II) ions at increasing concentrations in the medium significantly reduced the MB adsorption capacity compared to the single-component system. The concentration of MB adsorbed at equilibrium increased with increasing MB concentrations but decreased significantly with increasing Pb(II) ion concentration. The maximum adsorbed MB concentration and adsorption capacity at equilibrium (the amount of MB adsorbed per unit weight of MHNTs-ALG at equilibrium), $q_{MB,eq.}$ (mg/g), were obtained as 252.70 mg/L and 434.65 mg/g in the medium containing 500 mg/L of MB and 50 mg/L of Pb(II) ions, respectively. The minimum adsorbed MB concentration and adsorption capacity at equilibrium were obtained as 46.11 mg/L and 79.32 mg/g in the medium

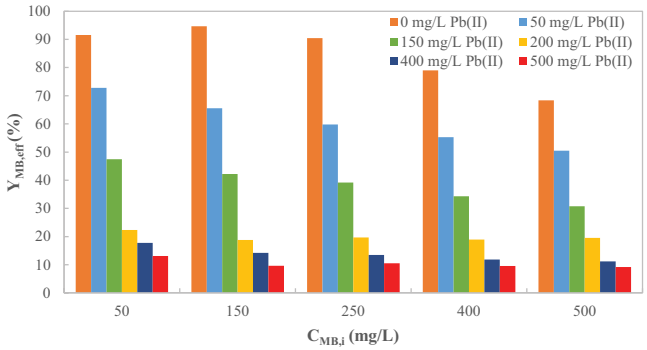

Fig. 4. The change in MB adsorption efficiency with the increasing initial MB concentration in media containing Pb(II) ions at different concentrations in the Pb(II)-MB binary adsorption system (temperature: 25°C, solution volume: 25 mL, pH: 5.0, adsorbent amount: 12.5 mg, MHNTs-ALG ratio: 1:2).

containing 500 mg/L of MB and 500 mg/L of Pb(II) ions, respectively.

Fig. 4 shows the change in MB equilibrium adsorption efficiency, $Y_{MB,eff.}$, with the increasing MB concentration in the medium containing 0, 50, 150, 250, 400, and 500 mg/L of Pb(II) ions. MB equilibrium adsorption efficiency decreased with the increasing concentration of Pb(II) ions and the increasing MB concentration. The highest MB adsorption efficiency was obtained as 72.76% in the medium containing 50 mg/L of Pb(II) ions and 50 mg/L of MB. This MB adsorption efficiency was lower than the adsorption efficiency of Pb(II) ions (88.45%) in the medium containing the same concentrations of Pb(II) and MB. The lowest MB adsorption efficiency was 9.21% in the medium containing 500 mg/L of Pb(II) and 500 mg/L of MB. This value was lower than the adsorption efficiency (24.86%) value obtained for Pb(II) ions in the medium containing the same concentrations of Pb(II) ions and MB.

Consequently, according to the results obtained from the binary system of Pb(II) ions and MB, as the concentration of MB dye increased, the adsorption capacity, adsorbed concentration, and adsorption efficiency of Pb(II) ions at equilibrium gradually decreased. Likewise, as the concentration of Pb(II) ions increased, the adsorption capacity, efficiency, and adsorbed concentration of MB dye at equilibrium decreased. In the single system of MB dye, its adsorption capacity by MHNTs-ALG hybrid beads, especially at high concentrations such as 400 and 500 mg/L, was higher than the adsorption capacity of single-component Pb(II) ions. On the other hand, in the Pb(II)-MB binary system, the decrease in the equilibrium adsorption capacity and efficiency of MB was greater compared to Pb(II) ions, which shows that the selectivity of Pb(II) ions was higher than that of MB in adsorption to MHNTs-ALG hybrid beads (data is shown Table S1).

4.1.2. Pb(II) ion-DB71 adsorption studies

To examine the adsorption of Pb(II) ions and anionic DB71 dye systems to MHNTs-ALG hybrid beads, the initial concentration of Pb(II) ions was increased in the range of 50–250 mg/L, whereas the concentration of DB71 dye

was kept constant at 0, 50, 100, 150, 200, and 250 mg/L in each adsorption medium. In these studies, beads with a 3:2 mass ratio of MHNTs to ALG, in which the single-component DB71 adsorption yielded the best results, were used to achieve selectivity for the anionic DB71 dye and increase the positive charge in MHNTs-ALG hybrid beads. Likewise, in single-component DB71 systems, 6.25 mg of hybrid beads were added to 25 mL of adsorption media at pH 3.0, where the highest DB71 adsorption capacity was obtained [41].

Fig. 5 shows the change in the concentration of Pb(II) ions adsorbed at equilibrium with the initial concentration of Pb(II) ions in media containing DB71 at increasing concentrations. The concentrations of Pb(II) ions adsorbed at equilibrium gradually decreased with the increasing DB71 concentration. This decrease in the concentrations of Pb(II) ions adsorbed at equilibrium results from the fact that the selected adsorption medium conditions (pH 3.0 and 3:2 mass ratio of MHNTs-ALG) were not the most appropriate conditions for the adsorption of Pb(II) ions. Moreover, since DB71 is an anionic dye, its inhibitory effect on the adsorption of Pb(II) ions is not so high. Pb(II) ions are selectively adsorbed at negatively charged centers on and inside MHNTs-ALG, a strong negatively charged matrix. On the other hand, the anionic DB71 dye binds to the positively charged alumina groups inside HNTs by electrostatic attraction forces. Therefore, the adsorption inhibition mechanism for Pb(II) ions and anionic DB71 dye should be considered non-competitive or partially competitive. For Pb(II) ions, the maximum adsorbed Pb(II) ion concentration and the adsorption capacity at equilibrium were obtained as 79.37 mg/L and 136.51 mg/g in the medium containing 250 mg/L of Pb(II) ions and 50 mg/L of DB71, respectively. The adsorbed concentration and adsorption capacity at equilibrium for Pb(II) ions decreased to 47.15 mg/L and 81.1 mg/g in the medium containing 250 mg/L of Pb(II)-250 mg/L of DB71, respectively.

Fig. 6 presents the change in Pb(II) equilibrium adsorption efficiency with the increasing Pb(II) concentration in media containing 0, 50, 100, 150, 200, and 250 mg/L of DB71. Pb(II) equilibrium adsorption efficiency decreased with the increasing Pb(II) ion and DB71 concentrations. Accordingly, the highest Pb(II) equilibrium adsorption efficiency was obtained as 62.74% in the medium containing 50 mg/L of Pb(II) and 50 mg/L of DB71. The lowest Pb(II) equilibrium adsorption efficiency was obtained as 18.5% in the medium containing 250 mg/L of Pb(II) and 250 mg/L of DB71. The reason for lower Pb(II) adsorption equilibrium capacity and efficiency than those obtained in the cationic MB dye system at approximately the same concentrations is that the adsorption conditions were not the most appropriate for the adsorption of Pb(II) ions, although Pb(II) ions were selectively adsorbed in the anionic DB71 dye system.

In the presence of Pb(II) ions at increasing concentrations, the concentrations of DB71 adsorbed at equilibrium, $C_{DB71,ads}$ mg/L, decreased significantly compared to its single-component system (Fig. 7). The concentration and adsorption capacity of DB71 adsorbed at maximum equilibrium in the medium containing 50 mg/L of Pb(II) and 250 mg/L of DB71 (the amount of DB71 adsorbed per MHNTs-ALG unit weight at equilibrium), $q_{DB71,eq.}$ (mg/g), were obtained as 26.50 mg/L and 91.16 mg/g, respectively. When the concentration of Pb(II) ions was increased to 250 mg/L in the medium containing 250 mg/L of DB71, the concentration and adsorption capacity of DB71 adsorbed at equilibrium decreased to 19.0 mg/L and 65.36 mg/g, respectively. DB71 equilibrium adsorption efficiency ($Y_{DB71,eff}$, %) also decreased significantly with the increasing concentrations of Pb(II) ions and DB71 compared to their single-component systems (Fig. 8). The highest DB71 equilibrium adsorption efficiency was obtained as 31.24% in the medium containing 50 mg/L of Pb(II) and 50 mg/L of DB71. This value was lower than the equilibrium adsorption efficiency (62.74%) value obtained for Pb(II) ions in the medium containing Pb(II) ions and DB71 at the same concentrations. The DB71 equilibrium adsorption efficiency decreased to 7.55% in the medium containing 250 mg/L of Pb(II) and 250 mg/L of DB71. This value was lower than the equilibrium adsorption efficiency (18.5%) value obtained for Pb(II) ions in the medium

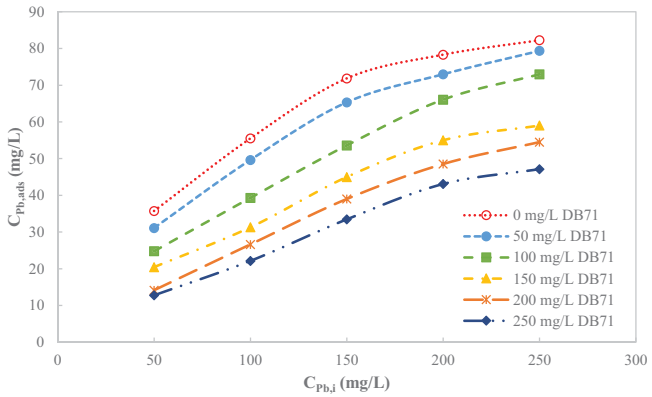

Fig. 5. The change in the Pb(II) ion concentration adsorbed at equilibrium with the increasing initial Pb(II) ion concentration in media containing DB71 at different concentrations in the Pb(II)-DB71 binary adsorption system (temperature: 25°C, solution volume: 25 mL, pH: 3.0, adsorbent amount: 6.25 mg, MHNTs-ALG mass ratio: 3:2).

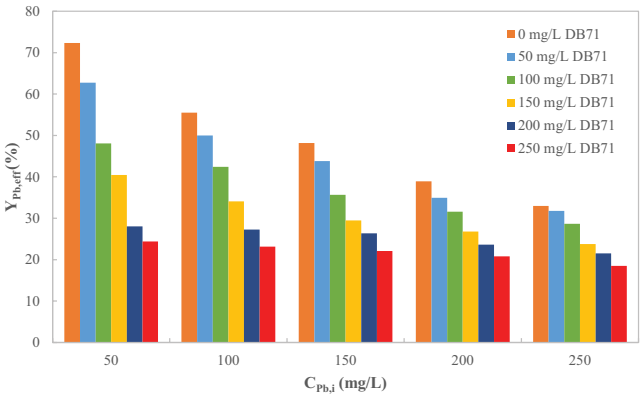

Fig. 6. The change in the equilibrium adsorption efficiency of Pb(II) ions with the increasing initial concentration of Pb(II) ions in media containing DB71 at different concentrations in the Pb(II)-DB71 binary adsorption system (temperature: 25°C, solution volume: 25 mL, pH: 3.0, adsorbent amount: 6.25 mg, MHNTs-ALG mass ratio: 3:2).

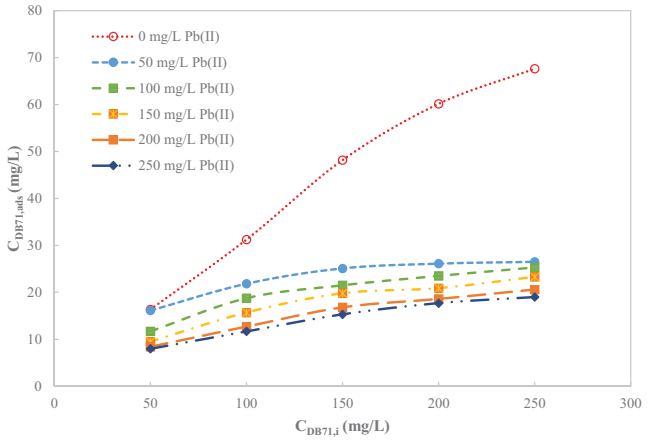

Fig. 7. The change in the DB71 concentration adsorbed at equilibrium with the increasing initial DB71 concentration in media containing Pb(II) ions at different concentrations in the Pb(II)-DB71 binary adsorption system (temperature: 25°C, solution volume: 25 mL, pH: 3.0, adsorbent amount: 6.25 mg, MHNTs-ALG mass ratio: 3:2).

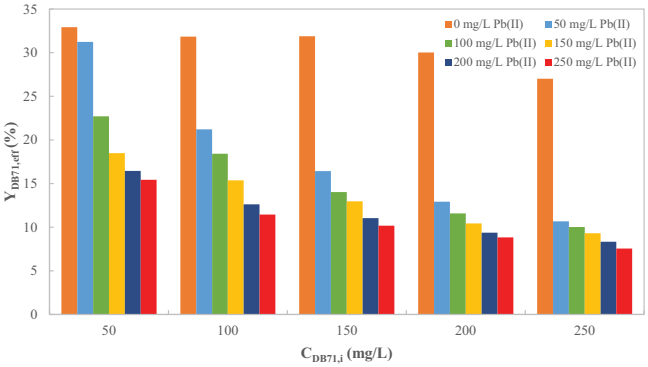

Fig. 8. The change in the equilibrium adsorption efficiency of DB71 with the increasing initial concentration of DB71 in media containing Pb(II) ions at different concentrations in the Pb(II)-DB71 binary adsorption system (temperature: 25°C, solution volume: 25 mL, pH: 3.0, adsorbent amount: 6.25 mg, MHNTs-ALG mass ratio: 3:2).

containing the same concentrations of Pb(II) ions and DB71. It was observed that Pb(II) ions were selectively adsorbed in the medium containing DB71 and Pb(II) ions together. Since Pb(II) exhibits cationic and DB71 exhibits anionic properties, they essentially bind to adsorption centers with different charges in the MHNTs-ALG matrix. However, DB71 and Pb(II) ions may decrease their adsorption capacities by interacting with each other ionically and electrostatically. Moreover, the type that binds to the MHNTs-ALG matrix may screen the binding of the other one. Pb(II) ions may selectively bind to negative centers on the matrix and prevent the matrix from strongly pushing the anionic DB71, which would be an inverse effect.

Fig. 9 comparatively presents equilibrium adsorption capacities (Pb(II), DB71, and MB amounts adsorbed per MHNTs-ALG unit weight at equilibrium, $q_{Pb,eq.}$, $q_{DB71,eq.}$, and $q_{MB,eq.}$, mg/g) in binary systems containing 50, 150, and

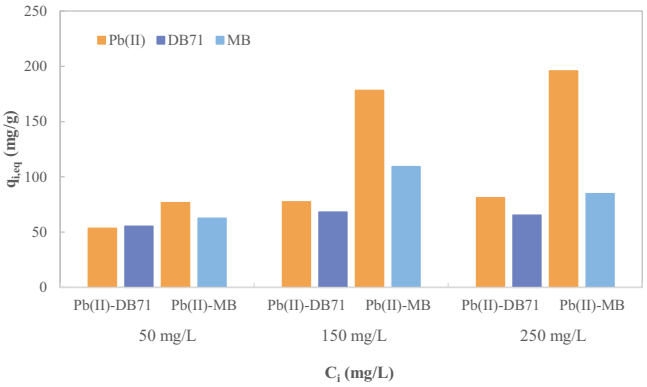

Fig. 9. Comparison of the Pb(II), DB71, and MB amounts adsorbed per unit adsorbent weight at equilibrium in media containing equal concentrations of Pb(II)-MB and Pb(II)-DB71 at the increasing initial Pb(II), MB, and DB71 concentrations in Pb(II)-dye binary systems.

250 mg/L of Pb(II)-DB71 and Pb(II)-MB at equal concentrations. The conditions for the Pb(II)-MB binary system (pH 5.0 and a 1:2 mass ratio of MHNTs to ALG) are optimal conditions for the adsorption of both Pb(II) ions and MB dye. Since both Pb(II) ions and MB dye are cationic, this is competitive adsorption for both of them. The outer surface of HNTs consists of a negatively charged silica layer, and the inner surface consists of a positively charged alumina layer. Furthermore, HNTs contain internal and external hydroxyl groups between their layers. Despite the small contribution of positive charges of alumina on the inner surface of HNTs, the potential of HNTs is negative between pH 2.0 and 12.0, similar to the surface potential of SiO_2. ALG is a negatively charged matrix when pH is higher than 3.4. ALG is negatively charged due to carboxyl groups in both ALG guluronic acid and mannuronic acid subunits in an aqueous solution. In the zeta potential measurements performed with the Malvern Nano ZS90 Zetasizer, the isoelectric pH value of MHNTs was measured as 2.89. MHNTs are negatively charged above this pH value. Since MHNTs-ALG hydrogels are strongly negatively charged above pH 3.0, they are expected to be strong adsorbents for both Pb(II) ions and cationic MB dye. Adsorption studies in single-component systems have revealed that MHNTs-ALG hydrogels exhibit the highest adsorption capacity for both Pb(II) ions and cationic MB dye at pH 5.0. Pb(II) and MB dye are first adsorbed on the surface of ALG beads. Afterward, they are absorbed by penetrating the beads and attach to the negatively charged silica outer surfaces of MHNTs. Meanwhile, they interact ionically with OH^- groups settled between the layers of MHNTs. In the medium containing 50 mg/L of Pb(II) and 50 mg/L of MB, the adsorption capacity was found to be 76.63 and 62.59 mg/g for Pb(II) and MB, respectively. When the concentration of both components was increased to 250 mg/L, the selectivity of Pb(II) ions increased significantly compared to cationic MB dye and reached 195.97 mg/g. The MB adsorption capacity in the same medium was 84.96 mg/g. In the presence of equal Pb(II) ion concentrations in the medium, the adsorption capacity of MB decreased significantly (Data was shown in Table S1).

On the other hand, it was aimed to achieve selectivity for the anionic DB71 dye by keeping the pH of the adsorption medium at 3.0 and increasing the mass ratio of MHNTs to ALG to 3:2. The anionic DB71 dye is assumed to be adsorbed into the inner luminal spaces of the tubular structure through electrostatic interaction with the positively charged alumina layer on the inner surface of MHNTs. Moreover, at lower pH values, such as pH 3.0, the negatively charged carboxylic acid groups of ALG biopolymers and the negatively charged silica groups of MHNTs are protonated with H^+ ions. Hence, H^+ ions start to compete with Pb(II) ions during adsorption. The anionic DB71 dye competes with Pb(II) ions for protonated centers and is adsorbed by the positively charged alumina layer inside the inner lumen of MHNTs. Thus, partial selectivity is achieved for DB71 dye with MHNTs-ALG beads, although it is a strong negatively charged matrix. Again, in the MHNTs-ALG matrix, the mass ratio of MHNTs to ALG was increased to 3:2, and the adsorption capacity of DB71 was increased. Since Pb(II) ions are cations and DB71 is an anionic dye, their binding to different adsorption centers in the MHNTs-ALG matrix indicates that adsorption occurs partially competitively or non-competitively. The adsorption capacities of Pb(II) and DB71 in the medium with 50 mg/L of Pb(II) and 50 mg/L of DB71 were 53.52 and 55.47 mg/g, respectively. In the medium with 250 mg/L of Pb(II) and 250 mg/L of DB71, the adsorption capacities of Pb(II) and DB71 were obtained as 81.10 and 65.36 mg/g, respectively (Data is shown in Table S2). MHNTs-ALG is a negatively charged matrix, and selectivity was achieved for DB71 despite cationic Pb(II) ions in the medium. The reason why the Pb(II) adsorption capacity is lower in the Pb(II)-DB71 binary system than in the Pb(II)-MB system, despite the presence of a strong competitive dye, MB, in the medium, is that the medium conditions (adsorption pH and MHNTs-ALG mass ratio) are not the optimum conditions for the adsorption of Pb(II) ions.

Fig. 10 comparatively presents equilibrium adsorption efficiencies (%) in binary systems containing 50, 150, and 250 mg/L of Pb(II)-DB71 and Pb(II)-MB at equal concentrations. The highest adsorption efficiency for Pb(II) ions was obtained as 88.45% in the medium containing 50 mg/L of Pb(II) and 50 mg/L of MB. In the same medium, MB adsorption efficiency was 72.76%. Pb(II) adsorption efficiency was 62.74% in the medium with 50 mg/L of Pb(II) and 50 mg/L of DB71. DB71 adsorption efficiency in the same medium was 31.24%.

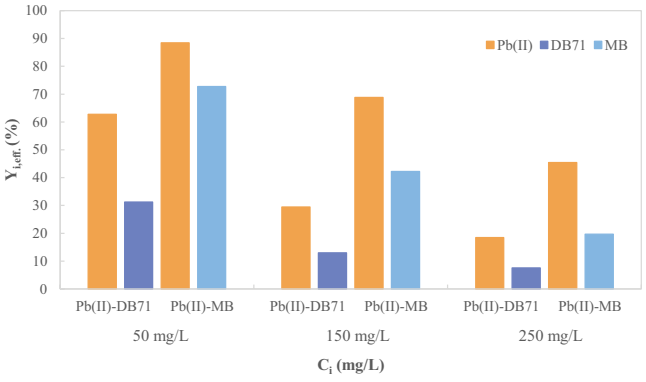

Fig. 10. Comparison of Pb(II), MB, and DB71 equilibrium adsorption efficiencies in media containing equal concentrations of Pb(II)-MB and Pb(II)-DB71 at the increasing initial Pb(II), MB, and DB71 concentrations in Pb(II)-dye binary systems.

4.2. Examination of the fit of the Pb(II)-MB binary adsorption system to the multi-component Langmuir model

The fit of the experimental equilibrium data of the Pb(II)-MB binary system to the multi-component Langmuir model given by Eq. (1) was investigated. Fig. 11 shows the multi-component Langmuir adsorption isotherms for the simultaneous adsorption of Pb(II) ions to MHNTs-ALG beads in the presence of MB concentrations increasing in the range of 50–500 mg/L. In the figures displaying the competitive adsorption equilibrium capacities of Pb(II) ions-MB, the multi-component Langmuir model profiles are shown with curves, whereas the symbols represent the values obtained experimentally. The four parameters of the Langmuir model, $K_{Pb,L}$, $q_{Pb,m}$, $K_{MB,L}$, and $q_{MB,m}$, were calculated using MS Excel 2019. The optimal values of the parameters were found by minimizing the sum of squared errors (SSE) and the total standard deviation (Table 1). Since Pb(II) ions and MB dye exhibit cationic properties, their binary adsorption system by MHNTs-ALG beads is competitive, and they compete with each other to attach to partially the same active centers of MHNTs-ALG beads or similarly charged centers. A higher value of the $K_{Pb,L}$ parameter obtained for Pb(II) ions than the value of the $K_{MB,L}$ parameter for MB indicates that the affinity of MHNTs-ALG beads for Pb(II) ions is higher compared to MB. A higher $K_{Pb,L}$ value of Pb(II) ions shows that the adsorption rate is higher than the desorption rate. Higher q_m values for both Pb(II) and MB demonstrate that the sorbent has a strong adsorption capacity for cationic Pb(II) and MB. Fig. 12 shows the multi-component Langmuir adsorption isotherms for the simultaneous adsorption of MB to MHNTs-ALG beads in the medium containing Pb(II) ions

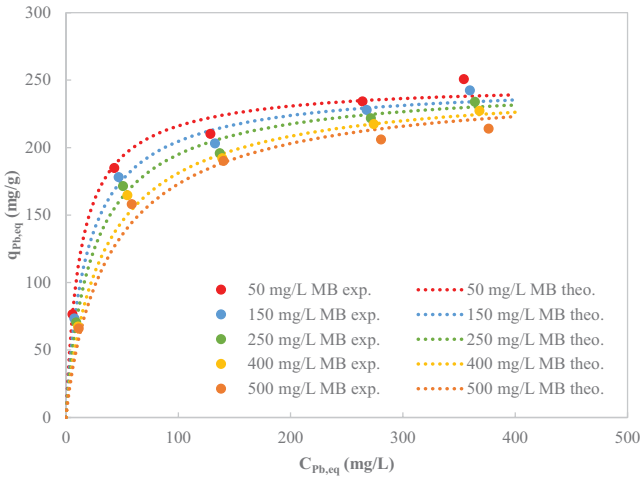

Fig. 11. Comparison of the experimental amounts of Pb(II) adsorbed at equilibrium per unit adsorbent weight with the theoretical isotherm curves obtained according to the multi-component Langmuir model in the presence of MB at increasing concentrations in Pb(II)-MB binary systems.

Table 1
The multi-component Langmuir model constants obtained in Pb(II)-MB binary systems (temperature: 25°C, solution volume: 25 mL, pH: 5.0, adsorbent amount: 12.5 mg, MHNTs-ALG ratio: 1:2)

Langmuir model	For Pb adsorption in the presence of constant concentrations of MB					For MB adsorption in the presence of constant concentrations of Pb				
$q_{Pb,m}$: 248.46 mg/g $K_{Pb,L}$: 0.0834 L/mg $q_{MB,m}$: 946.92 mg/g $K_{MB,L}$: 0.0068 L/mg	MB: 50 mg/L	MB: 150 mg/L	MB: 250 mg/L	MB: 400 mg/L	MB: 500 mg/L	Pb: 50 mg/L	Pb: 150 mg/L	Pb: 250 mg/L	Pb: 400 mg/L	Pb: 500 mg/L
EABS	6.89	6.64	6.68	5.56	6.5	7.74	9.07	8.6	5.52	3.02
ARE	2.48	3.28	3.84	3.16	3.14	3.69	6.27	10.67	10.22	8.19
ARSE	0.0387	0.0443	0.054	0.0447	0.0415	0.0594	0.0825	0.1507	0.1433	0.1142
R^2	0.983	0.988	0.989	0.99	0.988	0.997	0.992	0.976	0.979	0.991

EABS – Average absolute error; ARE – average relative error; ARSE – average relative standard error.

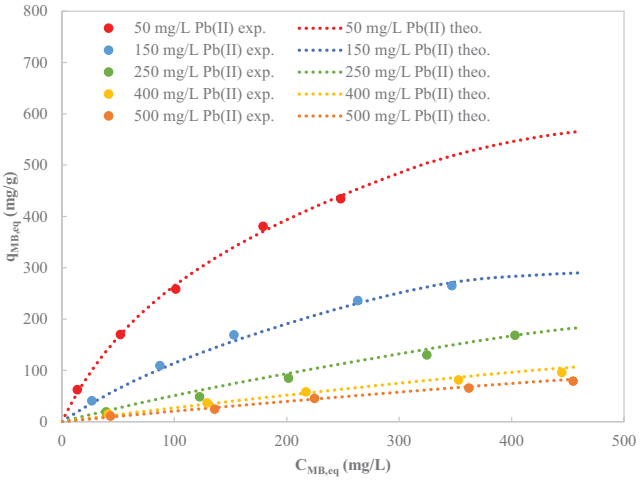

Fig. 12. Comparison of the experimental amounts of MB adsorbed at equilibrium per unit adsorbent weight with the theoretical isotherm curves obtained according to the multi-component Langmuir model in the presence of Pb(II) at increasing concentrations in Pb(II)-MB binary systems.

in the range of 50–500 mg/L. When the surface of MHNTs-ALG beads is coated with a single layer of MB, the amount of MB adsorbed per unit sorbent weight, $q_{MB,m}$, is higher than the $q_{Pb,m}$ value of Pb(II) ions. However, a high increase in the concentration of Pb(II) ions competing for the partially same adsorption centers in the medium significantly reduced the MB adsorption capacity. Since MHNTs-ALG beads have a finite number of binding centers, the equilibrium removal is expected to exhibit saturation kinetics characterized by the Langmuir model at high Pb(II) and MB dye concentrations, which was observed. Non-linearity in adsorption isotherms may arise from the saturation of centers adsorbing Pb(II) and MB and the interference between concentrated components competing for adsorption centers. Pb(II) ions significantly decreased MB adsorption by being adsorbed more quickly to active centers on MHNTs-ALG beads. Pb(II) ions that were first attached to the negatively charged centers may have activated repulsive forces for the binding of the cationic MB and screened the binding centers. The experimental points foreseen by the multi-component Langmuir model for both Pb(II) and MB usually deviate little. Considering both R^2 values and average relative error (ARE, %) values, it is seen that the equilibrium adsorption data of Pb(II) ions fit the multi-component Langmuir model better. However, since the amounts of MB adsorbed per MHNTs-ALG unit weight at equilibrium, $q_{MB,eq.}$, were low at high Pb(II) concentrations, the average relative error (ARE, %) between the experimental and predicted $q_{MB,eq.}$ values for MB increased.

As seen in the multi-component Langmuir adsorption isotherms, the amounts of both Pb(II) and MB adsorbed at equilibrium per unit adsorbent weight, $q_{Pb,eq.}$ and $q_{MB,eq.}$, decreased with the increasing concentrations of the other component. The equilibrium adsorption capacities of both components in the mixture were lower than their single-component systems. Furthermore, the total adsorbed MB and Pb(II) concentrations were higher than the adsorbed concentrations of the single-component Pb(II) system and lower than the adsorbed concentrations of the single-component MB system (Data is shown in Table S1). A similar trend was observed in the case of the total amounts, $q_{t,eq}$, adsorbed at equilibrium per unit weight of MHNTs-ALG beads. Although the individual effects of Pb(II) and MB were antagonistic in comparison with their single-component systems, the cumulative effects of their co-presence created a synergistic effect on the total adsorption capacity of MHNTs-ALG beads, $q_{t,eq}$, compared to the single-component Pb(II) system. In other words, the active surface centers of MHNTs-ALG beads are used more effectively in the case of multiple components. Nevertheless, the individual MB adsorption capacity of MHNTs-ALG beads was higher than the Pb(II)-MB system. In other words, the co-presence of Pb(II) ions and MB creates an antagonistic effect in terms of MB adsorption. For example, the $q_{Pb,eq.}$ and $q_{MB,eq.}$ values of MHNTs-ALG beads in the medium with 250 mg/L of Pb(II) and 250 mg/L of MB alone were 222.16 and 428.24 mg/g, respectively. In the medium with 250 mg/L of Pb(II) and 250 mg/L of MB, $q_{Pb,eq.}$, $q_{MB,eq.}$, and $q_{t,eq}$ values were 195.97, 84.96, and 280.17 mg/g, respectively. The increasing total concentration of MB and Pb(II) ions in the aqueous medium increased the metal-dye concentration difference on the surface and inner parts of MHNTs-ALG beads, and $q_{t,eq}$ values increased with the increasing driving force. The presence

of Pb(II) ions in the medium created a severe inhibitory effect on MB adsorption. Even a component not selectively adsorbed in the medium at increasing concentrations may mask the selectively adsorbed component. The screening effect of the second component in the adsorption medium may show a mixed synergistic and antagonistic effect on adsorption. In other words, the screening effect of the second component may induce synergism by mutually improving their individual repulsive forces and masking antagonism.

4.3. Examination of the fit of the Pb(II)-DB71 binary adsorption system to the multi-component Langmuir model

The fit of the partially competitive or non-competitive adsorption of DB71 and Pb(II) ions to MHNTs-ALG beads to the multi-component Langmuir model was examined. Figs. 13 and 14 show the isotherms obtained for Pb(II) and DB71, respectively, in the presence of increasing concentrations of the other component. Table 2 contains the constants calculated using the multi-component Langmuir model, $K_{Pb,L}$, $q_{Pb,m}$, $K_{DB71,L}$, and $q_{DB71,m}$. Since DB71 is an anionic dye, the active binding centers of MHNTs-ALG beads, especially the positively charged inner lumens of HNTs, are used more effectively in the presence of Pb(II) ions compared to two competitive cationic components, MB and Pb(II). The maximum adsorption capacity obtained when the surface of MHNTs-ALG beads was coated with a single layer of Pb(II) ions, $q_{Pb,m}$, was higher than the maximum adsorption capacity of DB71, $q_{DB71,m}$, despite the absence of optimum pH and MHNTs-ALG mass ratio for the adsorption of Pb(II) ions. $K_{i,L}$ values calculated from the model for Pb(II) and DB71 were also found to be extremely close to each other, indicating that MHNTs-ALG beads bind Pb(II) and DB71 with an affinity of approximately the same size, although their active centers binding Pb(II) and DB71 differ due to their surface charges.

The multi-component Langmuir model represents the equilibrium adsorption values of both Pb(II) ions and DB71 very well. The R^2 values obtained for Pb(II) ions are usually

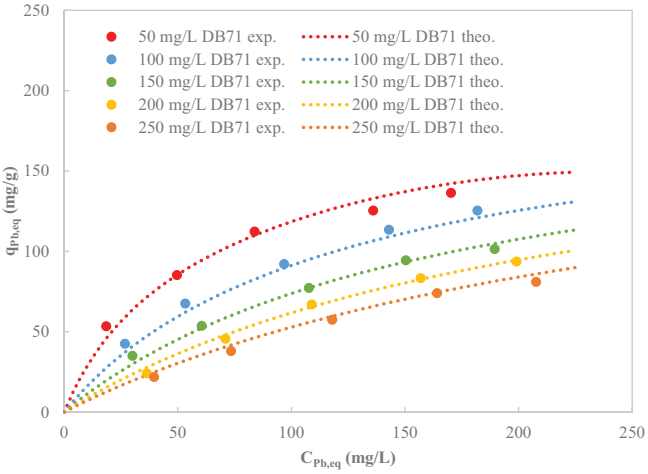

Fig. 13. Comparison of the experimental Pb(II) amounts adsorbed at equilibrium per unit adsorbent weight with the theoretical isotherm curves obtained according to the multi-component Langmuir model in the presence of DB71 at increasing concentrations in Pb(II)-DB71 binary systems.

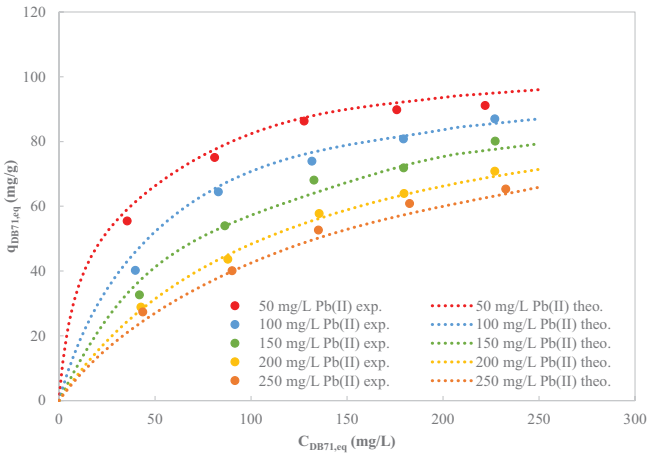

Fig. 14. Comparison of the experimental DB71 amounts adsorbed at equilibrium per unit adsorbent weight with the theoretical isotherm curves obtained according to the multi-component Langmuir model in the presence of Pb(II) at increasing concentrations in Pb(II)-DB71 binary systems.

Table 2
The multi-component Langmuir model constants obtained in Pb(II)-DB71 binary systems (temperature: 25°C, solution volume: 25 mL, pH: 3.0, adsorbent amount: 6.25 mg, MHNTs-ALG mass ratio: 3:2)

Langmuir model	For Pb adsorption in the presence of constant concentrations of DB71					For DB71 adsorption in the presence of constant concentrations of Pb				
$q_{Pb,m}$: 203.14 mg/g $K_{Pb,L}$: 0.0436 L/mg $q_{DB71,m}$: 118.96 mg/g $K_{DB71,L}$: 0.0501 L/mg	DB71: 50 mg/L	DB71: 100 mg/L	DB71: 150 mg/L	DB71: 200 mg/L	DB71: 250 mg/L	Pb: 50 mg/L	Pb: 100 mg/L	Pb: 150 mg/L	Pb: 200 mg/L	Pb: 250 mg/L
EABS	5.84	5.45	2.74	2.19	3.31	3.38	2.75	2.99	1.44	2.57
ARE	5.38	5.69	4.12	4.93	6.77	3.6	4.3	4.74	2.33	4.68
ARSE	0.0821	0.0708	0.0685	0.0857	0.0956	0.0451	0.0743	0.0741	0.0278	0.0648
R^2	0.975	0.978	0.99	0.991	0.982	0.954	0.961	0.96	0.993	0.973

EABS – Average absolute error; ARE – average relative error; ARSE – average relative standard error.

higher than the R^2 values for DB71. However, the average relative error (ARE, %) values obtained for DB71 are lower than the average relative error values calculated for Pb(II) ions.

Increasing the concentrations of Pb(II) and DB71 in binary mixtures between 50–250 mg/L gradually decreased the adsorption capacity of both components in the mixture in comparison with their single-component systems. As the concentration of the other component in the mixture was increased, the equilibrium adsorption capacity of Pb(II) and DB71 decreased. The total adsorbed concentrations of Pb(II) ions and DB71 two-component systems were higher than both the single-component Pb(II) and single-component DB71 systems (Data is shown in Table S2). Therefore, the co-presence of Pb(II) and DB71 created a synergistic effect on the adsorption capacity of MHNTs-ALG beads. However, increasing the DB71 concentration above 150 mg/L in the medium reduced the total amount of Pb(II) and DB71 adsorbed at equilibrium per unit sorbent weight, $q_{t,eq}$, below the equilibrium adsorption capacity of DB71 alone. In other words, in terms of DB71 adsorption, the co-presence of Pb(II) ions and DB71 created an antagonistic effect at DB71 concentrations higher than 150 mg/L. For example, $q_{Pb,eq.}$ and $q_{DB71,eq.}$ values of MHNTs-ALG beads in the medium with 250 mg/L of Pb(II) and 250 mg/L of DB71 alone were 141.48 and 232.69 mg/g, respectively. In the medium with 250 mg/L of Pb(II) and 250 mg/L of MB, $q_{Pb,eq.}$, $q_{MB,eq.}$, and $q_{t,eq}$ values were 81.1, 65.36, and 146.46 mg/g, respectively. The increasing total concentration in binary systems results in a strong repulsive force or a large difference in the concentration between the adsorbent surface and inner parts and solution, leading to higher adsorption of the components. The most possible explanation of this observed synergy is that various ligands on the surface and inner parts of MHNTs-ALG beads exhibit different affinity for DB71 and Pb(II) due to the surface charges of Pb(II) and DB71, and therefore the components bind to separate active centers. Although the amounts of Pb(II) ions and DB71 adsorbed alone decrease in comparison with their single-component systems and with the increasing concentrations of the other component, an increase in their total adsorbed amounts indicates that the surface and inner parts of MHNTs-ALG beads, especially the positively charged inner luminal spaces, are used more effectively in the two-component system.

Table 3 compares the maximum adsorption capacities obtained in the adsorption of single and Pb(II)-MB binary systems to various adsorbents. It has been noted that the presence of Pb(II) ions in wastewater has a synergistic effect on MB adsorption in the simultaneous adsorption of Pb(II) and MB on the sand coated with modified graphite oxide from their binary mixtures [34]. This study reported that the adsorption capacity of MB increased from 55.33 to 71.5 mg/g in the presence of Pb(II) ions. The presence of MB in the medium has an antagonistic effect on the adsorption capacity of Pb(II) ions. Anaerobic granular sludge was used for the simultaneous adsorption of Pb(II)-MB, and it was concluded that the co-presence of Pb(II) ions and MB created an antagonistic effect on the competitive adsorption capacity of both [35]. In the adsorption of the Pb(II)-MB binary system on nanomagnetic activated carbon, the observed effect is antagonistic as the maximum adsorption capacity of MB is reduced in the presence of Pb(II) ions [33]. Since no conclusion was reached about the adsorption capacity of the single-component Pb(II) system on nanomagnetic activated carbon in this study, no comment can be made about the effect of MB on Pb(II) adsorption. In both the single-component Pb(II) and MB systems and binary mixtures of MHNTs-ALG beads developed in our study, the adsorption capacities of Pb(II) and MB

Table 3
Comparison of the maximum Pb(II) and MB adsorption capacities of MHNTs-ALG beads in single and binary systems with other sorbents in the literature

Adsorbent	Adsorption capacity Pb(II) (mg/g)	Adsorption capacity MB (mg/g)	Competitive adsorption capacity Pb(II) (mg/g)	Competitive adsorption capacity MB (mg/g)	Operating conditions
Graphite oxide coated sand [34]	46.83	55.33	26.97	71.50	pH = 4.2, T = 25°C, C_i = 100–300 mg/L
Anaerobic granular sludge [35]	97.49	86	78.53	68.88	pH = 6.0, T = 25°C, C_i = 50–500 mg/L
Magnetic wood based activated carbon [33]	–	434.13	52.11	175.39	pH = 7.0, T = 25°C, C_i = 10–100 mg/L
Magnetic carbonate hydroxyapatite/ graphene oxide [30]	277.7	546.4	~271.0 ($Y_{eff.}$ = %97.59)	~528.04 ($Y_{eff.}$ = %96.64)	pH_{Pb} = 4.5, pH_{MB} = 9.1, T = 45°C, $C_{i,Pb}$ = 40–200 mg/L, $C_{i,MB}$ = 30–300 mg/L
Starch-lignosulfonate composite [44]	–	–	70.72	81.52	pH = 5.0, T = 25°C, C_i = 10–400 mg/L
Magnetic halloysite nanotubes-alginate In this study	274.37	659.92	250.90	434.65	pH = 5.0, T = 25°C, C_i = 50–500 mg/L

Table 4
Comparison of the maximum Pb(II) and DB71 adsorption capacities of MHNTs-ALG beads in single and binary systems with other sorbents in the literature

Adsorbent	Adsorption capacity Pb(II) (mg/g)	Adsorption capacity DB71 (mg/g)	Partially competitive adsorption capacity Pb(II) (mg/g)	Partially competitive adsorption capacity DB71 (mg/g)	Operating conditions
Food waste compost [32]	–	95.4	–	–	pH = 3.0, T = 50°C, C_i = 5–400 mg/L
Wheat shells (WS) [3]	–	46.30	–	–	pH = 6.0–8.0, T = 40°C, C_i = 50–500 mg/L
Pistachio hull waste (PHW) [26]	–	90.48	–	–	pH = 2.0, T = 50°C, C_i = 10–100 mg/L
Multi-walled carbon nanotubes (MWCNTs) [45]	–	3.42	–	–	pH = 3.0, T = 25°C, C_i = 25–100 mg/L
Cotton pod ash [46]	–	71.06	–	–	pH = 2.0, T = 50°C, C_i = 10–100 mg/L
Magnetic halloysite nanotubes-alginate In this study	141.48	232.69	136.51	91.16	pH = 3.0, T = 25°C, C_i = 50–250 mg/L

were considerably higher than the other adsorbents developed. Although both components compete robustly for the same centers of MHNTs-ALG beads and the individual effects of their co-presence are antagonistic, the adsorption capacities in mixtures are higher than the capacities of other adsorbents to adsorb MB and Pb(II) ions alone.

The adsorption of MB from single and binary component systems with various modified composite adsorbents was also investigated in the presence of other metal ions in the medium. Chen et al. [42] prepared an eco-friendly polydopamine composite adsorbent (CD-CA/PDA) based on cyclodextrin polymer and used it to remove cationic dyes and metals [42]. The adsorption capacity of CD-CA/PDA for MB and Cu(II) ions was found to be 582.95 mg/g (1.82 mmol/g) and 73.64 mg/g (1.16 mmol/g), respectively. The adsorption of MB was not affected by the presence of Cu(II) ions. It was reported that MB could be adsorbed by the cyclodextrin cavity by forming the host-guest inclusion complex despite the depletion of the negative groups. On the other hand, the amount of Cu(II) ions adsorbed decreased in the presence of MB due to the exhaustion of the negative groups. A citric acid crosslinked β-cyclodextrin polymer (CA-β-CD) prepared by Huang et al. was used for the simultaneous adsorption of MB and Cu(II) [43]. In single-component systems, heterogeneous maximum adsorption capacity values (q_m) of 0.9229 mmol/g (295.19 mg/g) and 0.9155 mmol/g (58.18 mg/g) were obtained for MB and Cu(II), respectively. In the MB-Cu(II) binary adsorption system, the MB adsorption capacity was obtained as 0.1339 mmol/g (42.83 mg/g), which was lower than the MB adsorption capacity (0.1549 mmol/g; 49.54 mg/g) in the system containing MB alone. On the other hand, the presence of MB clearly inhibited Cu(II) uptake, lowering single-component Cu(II) uptake capacity from 0.4916 mmol/g (31.23 mg/g) to 0.3838 mmol/g (24.39 mg/g) in the binary system. The adsorption s of MB and Cu(II) were inhibited by the presence of each other, suggesting the competition between the two cationic pollutants over the same adsorption sites. A proposed adsorption mechanism was that the carboxyl groups on the polymer surface instead of the cyclodextrin cavities were the main binding sites for polar MB and Cu(II) ions. This study demonstrated that the adsorption capacity of MB with MHNTs-ALG hybrid beads from single-component and binary-component systems was higher than the adsorption capacity of MB obtained with most adsorbents published in the literature (Table 3).

No studies examining the partial competitive adsorption of Pb(II)-DB71 binary mixture have been encountered in the literature. Table 4 compares the results obtained in a few studies investigating the adsorption of the single-component DB71 system by various adsorbents with the results acquired with MHNTs-ALG beads. The adsorption capacity of single-component DB71 dye with MHNTs-ALG beads is substantially higher than that of other adsorbents. Even in the presence of Pb(II) ions that immediately adhere to the strong negative matrix in the medium, the maximum capacity obtained for DB71 is higher than that of other adsorbents to adsorb only DB71 dye.

5. Conclusions

The individual adsorption capacity and efficiencies of Pb(II) ions and MB with MHNTs-ALG beads in binary mixtures are lower than single-component Pb(II) and MB systems. Furthermore, the total equilibrium adsorption capacity of Pb(II) ions and MB in binary systems, $q_{total,eq}$, is higher than the single-component Pb(II) system but lower than the single-component MB system. Therefore, it was concluded that the co-presence of Pb(II) and MB created a synergistic effect compared to the adsorption of Pb(II) ions alone and an antagonistic effect compared to the adsorption of MB. Pb(II) ions were observed to be selectively adsorbed in adsorption media containing Pb(II) ions and MB at equal concentrations.

On the other hand, since Pb(II) ions and DB71 were attached to different active centers of MHNTs-ALG or oppositely charged centers, the active surface area of the sorbent was used more effectively. The individual adsorption capacities and efficiencies of Pb(II) ions and DB71 decreased with the increasing concentrations of the other component in binary systems. However, the total equilibrium adsorption capacity of MHNTs-ALG beads increased compared to single-component Pb(II) and DB71 systems. When the concentration of DB71 in the mixture was increased above 150 mg/L, the total adsorption capacity decreased compared to the single-component DB71 system. Accordingly, it was concluded that the co-presence of Pb(II) and DB71 created a synergistic effect in comparison with the individual presence of Pb(II) ions and an antagonistic-synergistic mixed effect in comparison with the individual presence of DB71.

The multi-component four-parameter Langmuir model was successfully used to characterize multiple interactions on the adsorption of Pb(II)-MB and Pb(II)-DB71 to MHNTs-ALG beads. In the binary Pb(II)-MB system, $a_{Pb(II)}$ and a_{MB} of the Langmuir parameter obtained for Pb(II) ions and MB were 20.7216 and 6.4391 L/g, respectively. These values indicate that Pb(II) ions were selectively adsorbed with high capacity in the Pb(II)-MB system. The $a_{Pb(II)}$ and a_{DB71} values of the Langmuir parameter found for Pb(II) ions and DB71 dye were 8.8569 and 5.9599 L/g, respectively. The conditions of the adsorption medium were adjusted to the optimum values for DB71 to achieve selectivity for DB71, an anionic dye, with MHNTs-ALG beads, a mostly negatively charged matrix. For DB71, the desired selectivity and high adsorption capacity were acquired, particularly at high concentrations in its binary mixtures. Thus, it was proven that the MHNTs-ALG negatively charged matrix could be used in the adsorption of an anionic dye, even in the presence of Pb(II) ions, a cation that competes robustly in the medium. Although the conditions of the adsorption medium were not the most appropriate for the adsorption of Pb(II) ions, Pb(II) ions were also observed to dominate binding in the presence of DB71 dye. Pb(II) ions were selectively adsorbed in adsorption media with equal concentrations of Pb(II) ions and DB71 dye.

Declaration of competing interest

The authors declare that they have no known competing financial interests or personal relationships that could have appeared to influence the work reported in this paper.

Acknowledgments

The authors would like to thank TUBITAK, the Scientific and Technical Research Council of Turkey, for the 2210-C program.

References

[1] L. Liu, Y. Wan, Y. Xie, R. Zhai, B. Zhang, J. Liu, The removal of dye from aqueous solution using alginate-halloysite nanotube beads, Chem. Eng. J., 187 (2012) 210–216.
[2] M. Zhao, P. Liu, Adsorption behavior of Methylene Blue on halloysite nanotubes, Microporous Mesoporous Mater., 112 (2008) 419–424.
[3] Y. Bulut, N. Gözübenli, H. Aydın, Equilibrium and kinetics studies for adsorption of Direct Blue 71 from aqueous solution by wheat shells, J. Hazard. Mater., 144 (2007) 300–306.
[4] Y. Liu, J. Jia, T. Gao, X. Wang, J. Yu, D. Wu, F. Li, Rapid, selective adsorption of Methylene Blue from aqueous solution by durable nanofibrous membranes, J. Chem. Eng. Data, 65 (2020) 3998–4008.
[5] M. Munir, M.F. Nazar, M.N. Zafar, M. Zubair, M. Ashfaq, A. Hosseini-Bandegharaei, S.U.-D. Khan, A. Ahmad, Effective adsorptive removal of Methylene Blue from water by didodecyldimethylammonium bromide-modified brown clay, ACS Omega, 5 (2020) 16711–16721.
[6] S. Asadi, S. Eris, S. Azizian, Alginate-based hydrogel beads as a biocompatible and efficient adsorbent for dye removal from aqueous solutions, ACS Omega, 3 (2018) 15140–15148.
[7] X. Gao, C. Guo, J. Hao, Z. Zhao, H. Long, M. Li, Adsorption of heavy metal ions by sodium alginate based adsorbent-a review and new perspectives, Int. J. Biol. Macromol., 164 (2020) 4423–4434.
[8] C.S.C. Chiew, P.E. Poh, P. Pasbakhsh, B.T. Tey, H.K. Yeoh, E.S. Chan, Physicochemical characterization of halloysite/alginate bionanocomposite hydrogel, Appl. Clay Sci., 101 (2014) 444–454.
[9] T. Gotoh, K. Matsushima, K. Kikuchi, Preparation of alginate-chitosan hybrid gel beads and adsorption of divalent metal ions, Chemosphere, 55 (2004) 135–140.
[10] S. Takka, A. Gürel, Evaluation of chitosan/alginate beads using experimental design: formulation and in vitro characterization, AAPS PharmSciTech, 11 (2010) 460–466.
[11] W. Wang, S. Fan, Y. Zhang, C. Fan, Z. Huang, H. Hu, Y. Qin, Fe^{3+}-bridged cellulose-alginate composite gel beads as stable and effective photo-fenton catalysts, ACS Appl. Polym. Mater., 3 (2021) 5696–5706.
[12] H. Chen, J. Zhao, J. Wu, H. Yan, Selective desorption characteristics of halloysite nanotubes for anionic azo dyes, RSC Adv., 4 (2014) 15389–15393.
[13] W. Jinhua, Z. Xiang, Z. Bing, Z. Yafei, Z. Rui, L. Jindun, C. Rongfeng, Rapid adsorption of Cr(VI) on modified halloysite nanotubes, Desalination, 259 (2010) 22–28.
[14] M. Massaro, R. Noto, S. Riela, Past, present and future perspectives on halloysite clay minerals, Molecules, 25 (2020) 4863, doi: 10.3390/molecules25204863.
[15] Y. Zhao, E. Abdullayev, A. Vasiliev, Y. Lvov, Halloysite nanotubule clay for efficient water purification, J. Colloid Interface Sci., 406 (2013) 121–129.
[16] C.S.C. Chiew, H.K. Yeoh, P. Pasbakhsh, K. Krishnaiah, P.E. Poh, B.T. Tey, E.S. Chan, Halloysite/alginate nanocomposite beads: kinetics, equilibrium and mechanism for lead adsorption, Appl. Clay Sci., 119 (2016) 301–310.
[17] Y. Wu, Y. Zhang, J. Ju, H. Yan, X. Huang, Y. Tan, Advances in halloysite nanotubes-polysaccharide nanocomposite preparation and applications, Polymers (Basel), 11 (2019) 987, doi: 10.3390/polym11060987.
[18] O. Owoseni, E. Nyankson, Y. Zhang, D.J. Adams, J. He, L. Spinu, G.L. McPherson, A. Bose, R.B. Gupta, V.T. John, Interfacial adsorption and surfactant release characteristics of magnetically functionalized halloysite nanotubes for responsive emulsions, J. Colloid Interface Sci., 463 (2016) 288–298.
[19] G. Polat, Y.S. Açıkel, Synthesis and characterization of magnetic halloysite-alginate beads for the removal of lead(II) ions from aqueous solutions, J. Polym. Environ., 27 (2019) 1971–1987.
[20] Q. Liu, J. Wang, C. Duan, T. Wang, Y. Zhou, A novel cationic graphene modified cyclodextrin adsorbent with enhanced removal performance of organic micropollutants and high antibacterial activity, J. Hazard. Mater., 426 (2022) 128074, doi: 10.1016/j.jhazmat.2021.128074.
[21] M.A. Al-Ghouti, R.S. Al-Absi, Mechanistic understanding of the adsorption and thermodynamic aspects of cationic Methylene Blue dye onto cellulosic olive stones biomass from wastewater, Sci. Rep., 10 (2020) 15928, doi: 10.1038/s41598-020-72996-3.
[22] E.N. El Qada, S.J. Allen, G.M. Walker, Adsorption of Methylene Blue onto activated carbon produced from steam activated

bituminous coal: a study of equilibrium adsorption isotherm, Chem. Eng. J., 124 (2006) 103–110.
[23] F. Hafeez, H. Farheen, F. Mahmood, T. Shahzad, M. Shahid, M. Iqbal, S. Rasul, H. Manzoor, S. Hussain, Isolation and characterization of a lead (Pb) tolerant *Pseudomonas aeruginosa* strain HF5 for decolorization of reactive red-120 and other azo dyes, Ann. Microbiol., 68 (2018) 943–952.
[24] M. Wawrzkiewicz, P. Bartczak, T. Jesionowski, Enhanced removal of hazardous dye form aqueous solutions and real textile wastewater using bifunctional chitin/lignin biosorbent, Int. J. Biol. Macromol., 99 (2017) 754–764.
[25] N. Mirzaei, A.H. Mahvi, H. Hossini, Equilibrium and kinetics studies of Direct Blue 71 adsorption from aqueous solutions using modified zeolite, Adsorpt. Sci. Technol., 36 (2018) 80–94.
[26] H. Biglari, N. Javan, R. Khosravi, A. Zarei, Direct Blue 71 removal from aqueous solutions by adsorption on pistachio hull waste: equilibrium, kinetic and thermodynamic studies, Iran. J. Health Sci., 4 (2016) 55–70.
[27] A. Mojiri, H. Aziz, Wastewater Engineering: Advanced Wastewater Treatment Systems, IJSR Publications, Penang, 2014.
[28] S. Velusamy, A. Roy, S. Sundaram, T. Kumar Mallick, A review on heavy metal ions and containing dyes removal through graphene oxide-based adsorption strategies for textile wastewater treatment, Chem. Rec., 21 (2021) 1570–1610.
[29] R.R. Elmorsi, S.T. El-Wakeel, W.A. Shehab El-Dein, H.R. Lotfy, W.E. Rashwan, M. Nagah, S.A. Shaaban, S.A. Sayed Ahmed, I.Y. El-Sherif, K.S. Abou-El-Sherbini, Adsorption of Methylene Blue and Pb^{2+} by using acid-activated *Posidonia oceanica* waste, Sci. Rep., 9 (2019) 3356, doi: 10.1038/s41598-019-39945-1.
[30] L. Cui, Y. Wang, L. Hu, L. Gao, B. Du, Q. Wei, Mechanism of Pb(II) and Methylene Blue adsorption onto magnetic carbonate hydroxyapatite/graphene oxide, RSC Adv., 5 (2015) 9759–9770.
[31] C.S. Nkutha, N.D. Shooto, E.B. Naidoo, Adsorption studies of Methylene Blue and lead ions from aqueous solution by using mesoporous coral limestones, S. Afr. J. Chem. Eng., 34 (2020) 151–157.
[32] K. Al-Zawahreh, Y. Al-Degs, M.T. Barral, R. Paradelo, Optimization of Direct Blue 71 sorption by organic rich-compost following multilevel multifactor experimental design, Arabian J. Chem., 15 (2022) 103468, doi: 10.1016/j.arabjc.2021.103468.
[33] H. Ebadollahzadeh, M. Zabihi, Competitive adsorption of Methylene Blue and Pb(II) ions on the nano-magnetic activated carbon and alumina, Mater. Chem. Phys., 248 (2020) 122893, doi: 10.1016/j.matchemphys.2020.122893.
[34] J.-L. Gong, Y.-L. Zhang, Y. Jiang, G.-M. Zeng, Z.-H. Cui, K. Liu, C.-H. Deng, Q.-Y. Niu, J.-H. Deng, S.-Y. Huan, Continuous adsorption of Pb(II) and Methylene Blue by engineered graphite oxide coated sand in fixed-bed column, Appl. Surf. Sci., 330 (2015) 148–157.
[35] L. Shi, D. Wei, H.H. Ngo, W. Guo, B. Du, Q. Wei, Application of anaerobic granular sludge for competitive biosorption of Methylene Blue and Pb(II): fluorescence and response surface methodology, Bioresour. Technol., 194 (2015) 297–304.
[36] K.Y. Foo, B.H. Hameed, Insights into the modeling of adsorption isotherm systems, Chem. Eng. J., 156 (2010) 2–10.
[37] X. Chen, M.F. Hossain, C. Duan, J. Lu, Y.F. Tsang, M.S. Islam, Y. Zhou, Isotherm models for adsorption of heavy metals from water - a review, Chemosphere, 307 (2022) 135545, doi: 10.1016/j.chemosphere.2022.135545.
[38] G. McKay, B. Al Duri, Prediction of multicomponent adsorption equilibrium data using empirical correlations, Chem. Eng. J., 41 (1989) 9–23.
[39] G.-N. Moroi, E. Avram, L. Bulgariu, Adsorption of heavy metal ions onto surface-functionalised polymer beads. I. Modelling of equilibrium isotherms by using non-linear and linear regression analysis, Water Air Soil Pollut., 227 (2016) 260, doi: 10.1007/s11270-016-2953-5.
[40] G. Polat, Y.S. Acikel, Synthesis of magnetic halloysite nanotube-alginate hybrid beads: use in the removal of Methylene Blue from aqueous media, Int. J. Food Biosyst. Eng., 5 (2017) 15–22.
[41] G. Polat, E. Turkes, Y. Sağ Açıkel, Investigation of Adsorption Kinetics and Equilibrium for Removal of Anionic Dye Direct Blue 71 from Aqueous Media Using Magnetic Halloysite Nanotubes-Alginate Beads, Insac Natural and Technology Sciences, Duvar Publications, İzmir, 2022, pp. 215–240.
[42] H. Chen, Y. Zhou, J. Wang, J. Lu, Y. Zhou, Polydopamine modified cyclodextrin polymer as efficient adsorbent for removing cationic dyes and Cu^{2+}, RSC Adv., 389 (2020) 121897, doi: 10.1016/j.jhazmat.2019.121897.
[43] W. Huang, Y. Hu, Y. Li, Y. Zhou, D. Niu, Z. Lei, Z. Zhang, Citric acid-crosslinked β-cyclodextrin for simultaneous removal of bisphenol A, Methylene Blue and copper: the roles of cavity and surface functional groups, J. Taiwan Inst. Chem. Eng., 82 (2018) 189–197.
[44] R. Chen, J. Cai, Q. Li, X. Wei, H. Min, Q. Yong, Co-adsorption behaviors and mechanisms of Pb(II) and Methylene Blue onto a biodegradable multi-functional adsorbent with temperature-tunable selectivity, RSC Adv., 10 (2020) 35636–35645.
[45] R.F. Fard, M.E.K. Sar, M. Fahiminia, N. Mirzaei, N. Yousefi, H.J. Mansoorian, N. Khanjani, S. Rezaei, S.K. Ghadiri, Efficiency of multi walled carbon nanotubes for removing Direct Blue 71 from aqueous solutions, Eurasian J. Anal. Chem., 13 (2018), doi: 10.20933/ejac/85010.
[46] A.A. Zarei, H. Biglari, A. Biglari, G. Ebrahimzadeh, M.R. Narooie, A. Yari, E. Mehrizi, M. Ahamadabadi, M.M. Baneshi, M. Mobini, The removal of blue 71 from aqueous solution using cotton pod ash, Pollut. Res., 36 (2017) 489–497.

Supporting information

Table S1
Comparison of Pb(II) and MB concentrations adsorbed at equilibrium, $C_{j,i}$, the amounts of Pb(II) and MB adsorbed at equilibrium per unit adsorbent weight, $q_{i,eq}$, Pb(II) and MB adsorption efficiencies, $Y_{i,eff.}$, and total amounts of Pb(II) and MB adsorbed at equilibrium per unit adsorbent weight, $q_{t,eq}$ in Pb(II)-MB binary systems (temperature: 25°C, solution volume: 25 mL, pH: 5.0, adsorbent amount: 12.5 mg, MHNTs-ALG ratio: 1:2)

$C_{Pb,i}$ (mg/L)	$C_{MB,i}$ (mg/L)	$C_{Pb,ads.}$ (mg/L)	$q_{Pb,eq.}$ (mg/g)	$Y_{Pb,eff.}$ (%)	$C_{MB,ads.}$ (mg/L)	$q_{MB,eq.}$ (mg/g)	$Y_{MB,eff.}$ (%)	$q_{t,eq}$
50	–	48.01	91.98	97.14	–	–	–	–
250	–	129.95	222.16	51.72	–	–	–	–
500	–	157.20	274.37	31.44	–	–	–	–
–	50	–	–	–	46.48	87.75	91.57	–
–	250	–	–	–	227.18	428.24	90.44	–
–	500	–	–	–	342.52	659.92	68.33	–
50	50	44.55	76.63	88.45	36.39	62.59	72.76	139.22
250	50	122.25	210.27	48.75	11.28	19.41	22.35	229.68
500	50	145.87	250.90	29.17	6.48	11.14	13.07	262.04
50	250	40.99	70.50	81.87	150.40	258.69	59.79	329.19
250	250	113.94	195.97	45.42	49.39	84.96	19.68	280.93
500	250	136.05	234.00	27.20	26.38	45.38	10.51	279.38
50	500	38.43	66.09	77.23	252.70	434.65	50.48	500.74
250	500	110.62	190.27	44.09	97.91	168.41	19.55	358.68
500	500	124.48	214.10	24.86	46.11	79.32	9.21	293.32

Table S2
Comparison of Pb(II) and DB71 concentrations adsorbed at equilibrium, $C_{i,ads.}$, the amounts of Pb(II) and DB71 adsorbed at equilibrium per unit adsorbent weight, $q_{i,eq}$, Pb(II) and DB71 adsorption efficiencies, $Y_{i,eff.}$, and total amounts of Pb(II) and DB71 adsorbed at equilibrium per unit adsorbent weight, $q_{t,eq}$ in Pb(II)-DB71 binary systems (temperature: 25°C, solution volume: 25 mL, pH: 3.0, adsorbent amount: 6.25 mg, MHNTs-ALG ratio: 3:2)

$C_{i,Pb}$ (mg/L)	$C_{i,DB71}$ (mg/L)	$C_{ads.,Pb}$ (mg/L)	$q_{eq.,Pb}$ (mg/g)	$Y_{ads.\ eff.,Pb}$ (%)	$C_{ads.,DB71}$ (mg/L)	$q_{eq.,DB71}$ (mg/g)	$Y_{ads.\ eff.,DB71}$ (%)	q_t
50	–	35.75	61.49	72.34	–	–	–	–
150	–	71.87	123.61	48.19	–	–	–	–
250	–	82.26	141.48	32.98	–	–	–	–
–	50	–	–	–	16.35	56.25	32.94	–
–	150	–	–	–	48.18	165.74	31.88	–
–	250	–	–	–	67.64	232.69	27.01	–
50	50	31.12	53.52	62.74	16.13	55.47	31.24	108.99
150	50	65.35	112.40	43.80	9.50	32.68	18.48	145.08
250	50	79.37	136.51	31.79	7.97	27.42	15.44	163.93
50	150	20.44	35.16	40.48	25.10	86.34	16.43	121.5
150	150	45.00	77.40	29.47	19.80	68.11	12.98	145.51
250	150	59.02	101.51	23.75	15.31	52.67	10.18	154.18
50	250	12.76	21.95	24.40	26.50	91.16	10.66	113.11
150	250	33.46	57.55	22.10	23.30	80.15	9.30	137.7
250	250	47.15	81.10	18.50	19.00	65.36	7.55	146.46